Available online at www.sciencedirect.com
SCIENCE DIRECT®
Journal of Organometallic Chemistry 689 (2004) 3612–3620
Journal of Organometallic Chemistry
www.elsevier.com/locate/jorganchem

Helices of ruthenium complexes involving pyridyl–azine ligands: synthesis, spectral and structural aspects

Sanjay K. Singh [a], Manish Chandra [a], D.S. Pandey [a,*], M.C. Puerta [b], Pedro Valerga [b]

[a] Department of Chemistry, Awadhesh Pratap Singh University, Rewa 486 003, Madhya Pradesh, India
[b] Departamento de Ciencia de los Materiales e Ingeniería Metalúrgica y Química Inorgánica, Facultad de Ciencias, Universidad de Cádiz, 11510 Puerto Real, Cádiz, Spain

Received 10 May 2004; accepted 18 August 2004
Available online 17 September 2004

Abstract

New cationic complexes $[Ru(\eta^5\text{-}C_5H_5)(EPh_3)(L)]BF_4$ [L = pyridine-2-carbaldehyde azine (paa); E = P, **1**; E = As, **2**; E = Sb, **3**] and κ^1 bonded dppm complexes $[Ru(\eta^5\text{-}C_5H_5)(\kappa^1\text{-dppm})(L)]BF_4$ [L = paa **4;** L = *p*-phenylene-bis(picoline)aldimine (pbp) **5**] containing both group V donor and pyridyl–azine ligand are reported. The complexes were fully characterized by analytical and spectral studies. ^{31}P NMR spectral studies suggested coordination of dppm in the complexes **4** and **5** in κ^1-manner, which was further, confirmed by structural studies on the representative complex **4**. Weak interaction studies revealed that inter- and intramolecular C–H···X (X = O, F, Cl, π) and π–π interactions in the complexes **1** and **4** lead to helical structures.

Keywords: Ruthenium; Pyridyl–azine; dppm; X-ray; Weak interactions

1. Introduction

Much attention has been paid towards development of hetero bimetallic systems because of their potential use as homogeneous catalysts [1]. In this regard, ruthenium compounds which can act as chemical oxidants of alcohol and catalyst for their electro-oxidation have drawn considerable current attention [2]. A number of hetero bimetallic complexes utilizing bridging ligands, especially, those based on κ^1 dppm, have been developed and extensively studied as a possible catalyst for methanol oxidation [3]. The most common strategy employed for the development of such systems, involve construction of the monomeric complexes with κ^1-bonded dppm, followed by introduction of the second metal from its suitable precursor [3a,4]. In the course of studies directed towards designing of new *metallo-ligands* based on organometallic systems, we have prepared new complexes $[Ru(\eta^5\text{-}C_5H_5)(EPh_3)(L)]BF_4$ [L = paa; E = P, **1**; E = As, **2**; E = Sb, **3**] and $[Ru(\eta^5\text{-}C_5H_5)(\kappa^1\text{-dppm})(L)]BF_4$ [L = paa **4;** L = *p*-phenylene-bis(picoline)aldimine (pbp) **5**]. Although, ruthenium complexes containing both V donor and poly–pyridyl ligands are reported in the literature, analogous complexes imparting both V donor and pyridyl–azine ligands are yet to be explored. The complexes containing both the group V donor and a pyridyl–azine ligand are being reported for the first time. Further, the complexes **1**, **2** and **3** bear uncoordinated donor sites on the paa, while the complexes **4** and **5** bears pendant P and N donor group from the dppm, pbp and paa. Thus, the complexes under study have the potential to behave as *metallo-ligands* and could find application in the development of homo/hetero bimetallic systems.

Importance of weak interactions viz. C–H···X (X = O, F, Cl, π) and π–π stacking between aromatic rings has widely been recognized for creation of self

* Corresponding author. Tel./fax: +91 7662 230684.
E-mail address: dsprewa@yahoo.com (D.S. Pandey).

0022-328X/$ - see front matter © 2004 Elsevier B.V. All rights reserved.
doi:10.1016/j.jorganchem.2004.08.026

assembled artificial architectures as well as stabilization and intercalation studies [5]. At the same time considerable attention has been paid towards weak interaction studies in organometallic systems [6]. The interaction studies on the complexes **1** and **4** revealed presence of weak inter- and intramolecular C–H···X (X = O, F, Cl, π) and π–π stacking between aromatic rings of the PPh_3 ligand. These interactions result in helical network in the complexes **1** and **4**. In this article we present synthetic, spectral, electrochemical, structural and weak interaction studies on the cationic complexes $[Ru(\eta^5\text{-}C_5H_5)(EPh_3)(L)]BF_4$ (L = paa; E = P, **1**; E = As, **2**; E = Sb, **3**) and $[Ru(\eta^5\text{-}C_5H_5)(\kappa^1\text{-dppm})(L)]BF_4$ (L = paa **4;** L = *p*-phenylene-bis(picoline)aldimine (pbp) **5**) containing both group V donor and pyridyl–azine ligands.

2. Results and discussion

2.1. Synthesis

Reactions of the complex $[Ru(\eta^5\text{-}C_5H_5)Cl(EPh_3)_2]$ (E = P, As or Sb) and the dppm complex $[Ru(\eta^5\text{-}C_5H_5)\text{-}(\kappa^2\text{-dppm})Cl]$ with N–N′ donor bases pyridine-2-carbaldehyde azine (paa) and *p*-phenylene-bis(picoline)aldimine (pbp) under refluxing conditions in methanol led in the formation of the cationic complexes **1**–**5** as shown in Scheme 1. The complexes **1**–**5** were isolated as their BF_4^- salts.

The complexes **1**–**5**, are air stable solids and do not show any signs of decomposition in solution upon exposure to air for days. Further, it was observed that in the reactions leading to formation of the complexes **1**–**3**, no intermediates were isolated. It is supposed that the reactions pass through intermediacy of the complexes derived by polarization of Ru–Cl bond and loss of one EPh_3 ligand followed by coordination of pyridyl–azine ligand through immine–azine nitrogen. To provide site for interaction of the pyridyl–azine ligands through its immine–azine nitrogen, it appears that during formation of the complexes $[Ru(\eta^5\text{-}C_5H_5)(\kappa^1\text{-dppm})(L)]BF_4$ from $[Ru(\eta^5\text{-}C_5H_5)(\kappa^2\text{-dppm})Cl]$ and N–N′ donor bases paa and pbp, κ^2-bonded dppm gets detached from one end and forms κ^1-bonded dppm complex. Presence of the κ^1-coordination mode of dppm has been confirmed by $^{31}P\{^1H\}$ NMR spectral studies on complexes (**4** and **5**) and structural studies on complex (**4**).

2.2. Characterization

The complexes were fully characterized by IR, NMR (^1H and ^{31}P), electronic, emission spectral and electrochemical studies. Analytical data of the complexes corroborated well to their respective formulation. Information about composition of the complexes was also obtained from FAB mass spectral studies and resulting data is recorded in Section 3. The presence of different peaks and their position in the FAB-MS spectra of the complexes conformed well to formulation of the respective complexes.

Infrared spectra of the complexes exhibited characteristic bands due to pyridyl ring vibrations of the ligand along with the characteristic bands associated with phenyl ring vibrations, Cp ring and counter anions. The ν_{C-N} band in the complexes shifted towards lower wave number and appeared around 1612 cm^{-1}, as compared to that in the free ligand (1638 cm^{-1}). The bands associated with pyridyl ring breathing mode appeared at ~1032 cm^{-1}. The shift in the position of ν_{C-N} and pyridyl ring breathing mode suggested co-ordination of the metal ion through pyridyl and diazine nitrogen [3b]. Broad bands in the region 1118 cm^{-1} have been assigned to counter anion BF_4^-.

^1H NMR spectral data of the complexes are recorded in Section 3 along with other data. In ^1H NMR spectra of the complexes Cp protons resonated as a sharp singlet, aromatic protons of EPh_3 as a broad multiplet and protons associated with paa and pbp resonated in

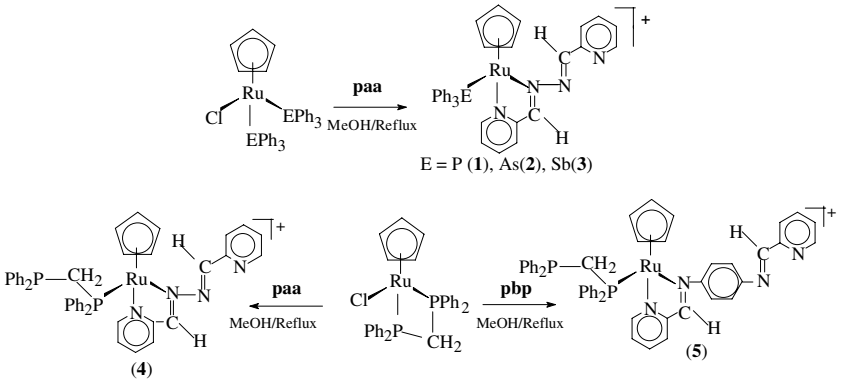

Scheme 1.

their usual position [7]. $^{31}P\{^1H\}$ NMR spectra of the complex **1** displayed a sharp singlet at δ 48.15 ppm corresponding to the coordinated ^{31}P nuclei. However, $^{31}P\{^1H\}$ NMR spectra of the dppm complexes **4** and **5** displayed two well separated resonance at −26.5 (d), 41.0 (d) and −27.5 (d), 42.6 (d) ppm, respectively. The downfield resonance (41.0 and 42.6 ppm) has been assigned to ruthenium bound phosphorus, while those in the up field side at −26.5 (d) and −27.5 (d) ppm to the pendant phosphorus. The presence of two well separated resonances in the $^{31}P\{^1H\}$ NMR spectra of the complexes **4** and **5**, suggested that the ^{31}P nuclei in these complexes are present in different chemical environments and dppm is acting as monodentate ligand. This observation is consistent with our earlier findings and has further been confirmed by single crystal X-ray diffraction studies [8].

The low spin d^6 orbitals on ruthenium provides filled metal orbitals of proper symmetry to interact with the relatively low lying π* orbitals on the ligand paa. It is expected to give a band associated with metal to ligand charge transfer (MLCT) transition ($t_1g \rightarrow \pi^*$) whose position varies with the nature of metal ion and the ligand acting as π acceptor. Electronic spectra of the complexes displayed bands in the region 416–470, 314–362 and 286–310 nm. The low energy band in the region 416–470 nm has been assigned to MLCT transition [Ru(II) → π* orbital of paa]. It was further observed, that the band associated with MLCT transition was sensitive to the polarity of the solvent and it showed a shift towards high-energy side with an increase in the dielectric constant of the solvent. Representative spectrum for the complex **4** is shown in Fig. 1. This shift may be attributed to the ground state stabilization or excited state destabilization of the complexes in solvents of high polarity [9]. The complexes **1**–**5** under study are cationic species and polar solvents are expected to stabilize the ground state of the complexes, which may be responsible for the observed results. Alternatively, the MLCT transition may induce a dipole moment in the excited state, which is directed antiparallel to that of the ground state dipole moment. This will generate a less polar situation in the excited state because of which the excited state is relatively less stabilized compared to ground state or destabilized by the polar solvents thereby causing negative solvatochromism in the complexes [10]. Besides the MLCT band, the electronic spectrum should also be characterized by π–π* transition. The non-solvatochromic bands in the range 286–310 nm has been assigned to intraligand π–π* transitions. The bands in the region 350–360 nm have been assigned to MLCT transitions from Ru (II)–π*-orbitals of the η^5-C_5H_5 ring.

Emission spectrum of the complex **1** was obtained in CH_2Cl_2 at room temperature and the resulting spectrum is shown in Fig. 2. Upon excitation at MLCT band it luminesce at 539 nm. The emission is intense and could not attributed to the free ligand. Further, the shape and position of the band indicated that it is due to ^{3}MLCT.

Cyclic voltammogram of the complexes **1**, **2**, **4** and **5** were recorded in purified acetonitrile and resulting data is summarized in (Table 1). On the anodic potential window (0 to +2 V vs SCE) complexes **1** (Fig. 3) and **2** exhibited quasi-reversible peaks at potential 0.98 and 0.97 V and the complexes **4** and **5** exhibited irreversible peaks at 1.12 and 1.55 V attributed to metal based oxidation Ru(II/III), respectively [3b,11]. On the other hand, on the cathodic potential window (0 to −2 V vs SCE), these complexes exhibited two (for paa) and three ligand (for pbp) based reduction couple. Reduction potential of the mononuclear complexes $[Ru^{II}(\eta^5\text{-}C_5H_5)(\kappa^1\text{-dppm})(\kappa^2\text{-paa})]^+$ (**4**) and $[Ru^{II}(\eta^5\text{-}C_5H_5)(\kappa^1\text{-dppm})(\kappa^2\text{-pbp})]^+$ (**5**) move anodically in the order

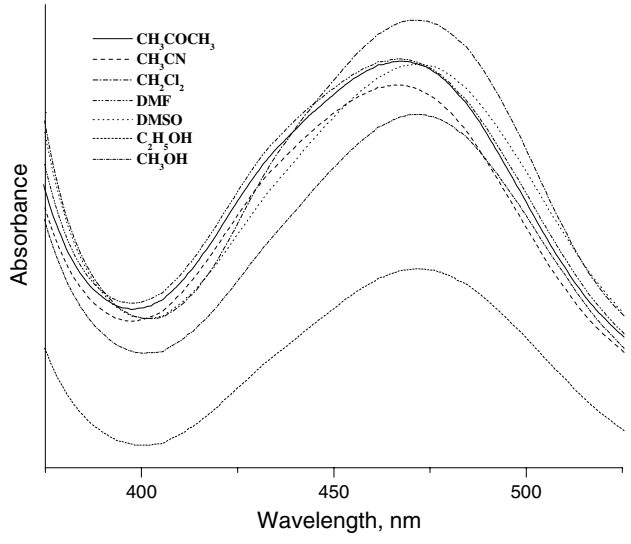

Fig. 1. Electronic spectra of the complex **4** in different solvents.

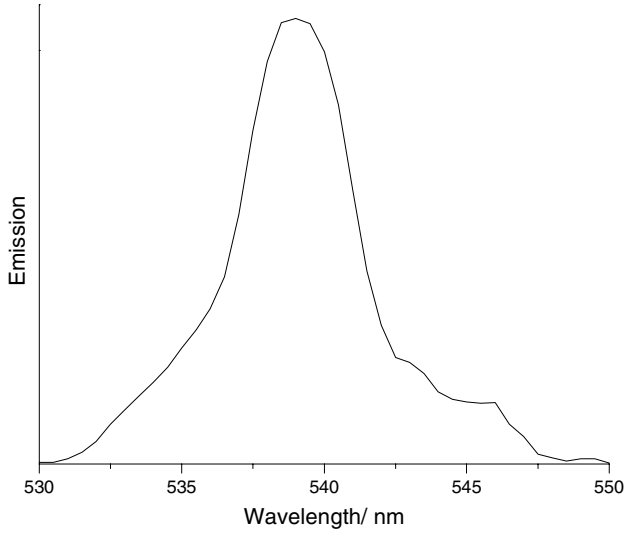

Fig. 2. Emission spectrum of the complex **1** in CH_2Cl_2 at room temperature.

Table 1
Electrochemical data for mono and binuclear Ru(II) complexes in acetonitrile solution at (rt), scan rate 50 mV s^{-1}

Complexes	Oxidation	Reduction		
	$E_{(1/2)}$	$E_{(1/2)}$	$E_{(1/2)}$	$E_{(1/2)}$
		I	II	III
$[Ru(\eta^5\text{-}C_5H_5)(PPh_3)(\kappa^2\text{-paa})]BF_4$ (**1**)	0.987(117)	−1.05(79)	−1.66(70)	–
$[Ru(\eta^5\text{-}C_5H_5)(AsPh_3)(\kappa^2\text{-paa})]BF_4$ (**2**)	0.973(125)	−1.10(91)	−1.69(110)	–
$[Ru(\eta^5\text{-}C_5H_5)(\kappa^1\text{-dppm})(\kappa^2\text{-paa})]BF_4$ (**4**)	1.12[a]	−1.09(112)	−1.71(80)	–
$[Ru(\eta^5\text{-}C_5H_5)(\kappa^1\text{-dppm})(\kappa^2\text{-pbp})]BF_4$ (**5**)	1.55[a]	−1.04(80)	−1.45(135)	–1.7[a]

$E_{(1/2)} = 0.5(E_{pa} + E_{pc})$, where E_{pa} and E_{pc} are the anodic and cathodic potential, respectively, the value of ΔE_p in (mV is given in parentheses), $\Delta E_p = E_{pa} - E_{pc}$.
[a] For irreversible peaks E_{pa}.

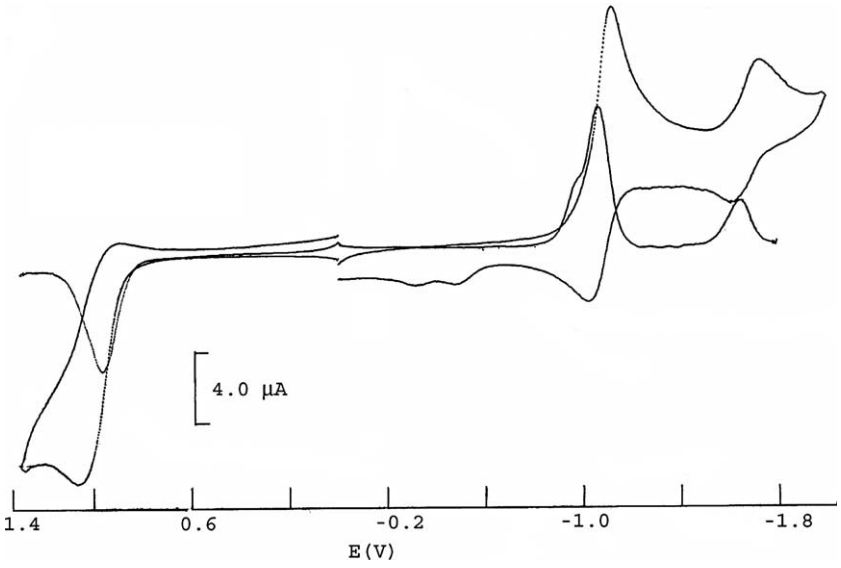

Fig. 3. Cyclic voltammogram of the complex **1** in acetonitrile.

L = paa < pbp, this reflects the lowering of LUMO energy of the ligand. Reduction potential peaks in the complexes are 0.5–0.7 V more positive than those of free ligands [12].

2.3. Molecular structure determination

Molecular structure of the representative complexes **1** and **4** was determined by single crystal X-ray diffraction analyses. Molecular representations of the complex cation of **1** and **4** are given in Figs. 4 and 5. Details about data collection, solution and refinement are recorded in Table 2 and selected bond lengths and bond angles are recorded in Table 3. Both the complexes have monoclinic crystal system with space group $P2_1/n$. The complexes **1** and **4** adopted typical three legged *piano stool* geometry about the metal center ruthenium. Average Ru–C distances in the complexes **1** and **4** are 2.187 and 2.176 Å, respectively, and Ru to centroid of Cp distances in complexes **1** and **4** are 1.838 and 1.829 Å,

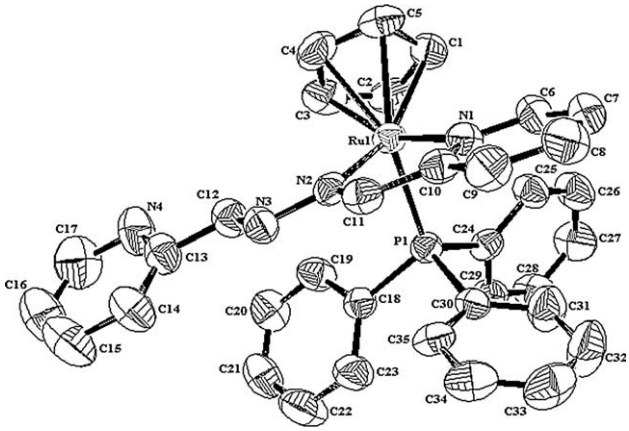

Fig. 4. Molecular representation of the complex **1**.

respectively [3b,13]. The Ru–C_{av} distances are comparable to those in other Ru–Cp complexes [14]. The Ru–P distances in both the complexes **1** and **4** are essentially

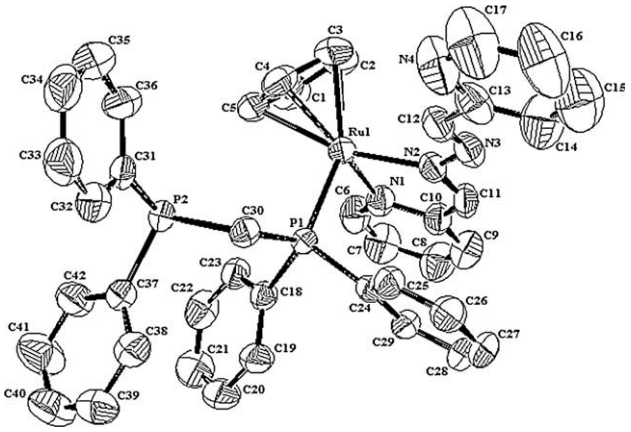

Fig. 5. Molecular representation of the complex **4.**

Table 2
Crystal data and data collection with refinement details for the complexes **1** and **4**

	Complex **1**	Complex **4**
Empirical formula	$C_{35}H_{30}N_4PRu$ 1+, BF_4 1−, H_2O	$C_{42}H_{37}N_4P_2Ru$ 1+, BF_4 1−
Molecular weight	743.50	847.58
Color and habit	Red, plate	Red, needle
Crystal size (mm)	$0.10 \times 0.16 \times 0.24$	$0.12 \times 0.24 \times 0.65$
Space group	$P2_1/n$ (no. 14)	$P2_1/n$ (no. 14)
System	Monoclinic	Monoclinic
Unit cell dimensions		
a (Å)	9.3737(8)	12.6147(16)
b (Å)	15.6496(14)	10.2617(13)
c (Å)	22.708(2)	30.605(4)
β (°)	97.452(2)	92.260(3)
V (Å^3)	3303.0(5)	3958.7(8)
Z	4	4
D_{calc} (g cm^{-3})	1.495	1.422
μ (mm^{-1})	0.581	0.531
Temperature (K)	293	293
No. of reflections	5790	7034
Total/unique data	24 413, 5790	28 919, 7034
$R_{(int)}$	0.089	0.035
No. of refined parameters	430	529
R, wR_2	0.0542, 0.1190	0.0739, 0.1555
Goodness-of-fit	0.995	1.051

Table 3
Selected bond lengths (Å), angles (°) and torsion angles (°) for the complexes **1** and **4**

	Complex **1**	Complex **4**
Ru1–N1	2.063(4)	2.081(5)
Ru1–N2	2.081(4)	2.080(4)
Ru1–P1	2.330(12)	2.343(13)
Ru1–$C_{av.}$	2.187	2.176
Ru1–Ct.	1.838	1.829
N1–Ru1–N2	76.33(15)	75.93(18)
N1–Ru1–P1	91.38(10)	91.76(13)
N2–Ru1–P1	89.04(10)	91.39(13)
C11–N2–N3–C12	−178.3	−168.7(5)

equal and are 2.330(12) and 2.343(13) Å, respectively, and these lies in the range as reported for Ru–P distances in other related systems [3b,13,15].

The Ru–N_{py} and Ru–N_{azine} bond distances and N–Ru–N bond angles are comparable in these complexes. In the complex **1**, the Ru–N_{azine} distance Ru–N(2) is 2.081(4) Å which is comparable to Ru–N_{py} distance Ru–N(1) which is 2.063(4) Å. In the complex **4** the Ru–N_{azine} and Ru–N_{py} distances essentially equal and are 2.081(5) and 2.080(4) Å, respectively, and fall in the same range as observed in other pyridyl azo complexes [16].

In the complex **1** the angle N(1)–Ru(1)–N(2) of 76.33(15)° suggested inward bending of the coordinated pyridyl and azine group. At the same time coordinated part of the paa ligand is planar, which is indicated by torsion angle N(2)–C(11)–C(10)–N(1), that is −3.0(6)°. Similarly, in the complex **4**, the angle N(1)–Ru(1)–N(2) is 75.93(18) and torsion angle N(1)–C(10)–C(11)–N(2) −1.5(8)°. Torsion angles C11–N2–N3–C12 and C11–N2–N3–C12 are −178.3° and −168.7(5)°, respectively, in the complexes **1** and **4** and suggested that paa ligand is almost planar in both the complexes. The N(2)–N(3) distances in complexes **1** and **4** are 1.411(5) and 1.416(7) Å, respectively, which is comparable to that in hydrazine N–N single bond distance of 1.47 Å. The C=N bond lengths N(2)–C(11) and N(3)–C(12) in both the complexes 1.288(6) and 1.258(6) Å (complex **1**) and 1.284(7) and 1.253(8) Å (complex **4**), respectively, which are comparable and can be considered to have double bond character.

Crystal structure of both the complexes **1** and **4** revealed extensive inter- and intramolecular C–H···F, C–H···π and edge-to-edge π–π interactions with the involvement of cyclopentadiene rings. Further it is almost clear that these types of interactions play an immense role for the construction of huge supramolecular architecture. The strength of a particular interaction depends on the donor/accepter molecules. Strong T shaped C–H···π (2.71 Å) interactions along with C–H···F interactions is inherent to the supramolecular helical network of the complex **1** (Fig. 6). Such interactions are resulted from crystal packing and analyzing the extended 3-dimensional assemblies. Such interactions can be assigned as van der Waal interactions as C–H···F and C–H···π distances are well within the vdW distances and are consistent with other similar reports [17]. The relevant interaction distances are summarized in Table 4.

An important feature of the crystal packing structure of the complex **1** relates to the π–π stacking of the phenyl rings plane of the dppm ligands with an interplanar distances of 3.39 Å (Fig. 7) A similar extended single helical motif has been visualized for the complex **4**, vide the intermediacy of C–H···π (2.90 Å) and edge-to-edge π–π interactions (2.99 Å) (Fig. 8).

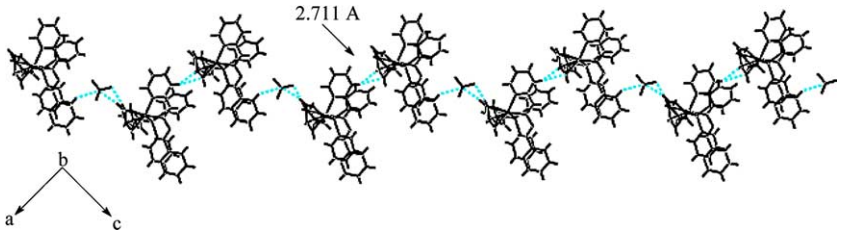

Fig. 6. Helical motif of the complex **1** accompanied by C–H···F and C–H···π interactions.

Table 4
Hydrogen bond distances (Å) and angles (°) for the complexes **1** and **4**

*Complex **1***				
D–H···A	d(D–H)	d(H···A)	d(D···A)	<(DHA)
C1–H1···F1[a]	0.93	2.34	3.271(6)	175.1
C26–H26···F2[a]	0.93	2.57	3.424(4)	152.5
C–14–H14···F2[b]	0.93	2.58	3.397(4)	145.7
C8–H8···F4[c]	0.93	2.47	3.187(6)	133.7
C14–H14···N3	0.93	2.62	2.874(6)	96.1
C9–H9···π [C2=C3]	0.93	2.71	3.397	133.1
Symmetry operations:	[a] $1-x, 1-y, 1-z$	[b] $1-x, 0.5+y, 1.5-z$	[c] $-x, 1-y, 1-z$	
*Complex **4***				
C6–H6···F4[a]	0.93	2.44	3.261	147.7
C9–H9···F3[b]	0.93	2.53	3.293	139.8
C11–H11···F2[b]	0.93	2.44	3.254	145.6
C14–H14···N3	0.93	2.543	2.813	97.07
Symmetry operations:	[a] $1+x, -1+y, z$	[b] $1+x, y, z$		

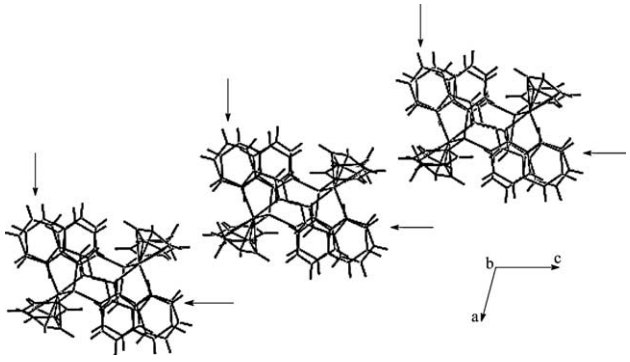

Fig. 7. Crystal packing of complex **1** shows face-to-face π–π stacking interactions (indicated by arrows).

2.4. Conclusion

In this work we have presented synthesis and characterization of new cationic ruthenium complexes involving both group V and pyridyl–azine ligands for the first time. The mononuclear complexes reported possessing uncoordinated donor sites from of paa, pbp and pendant donor group in the κ^1-dppm bonded complexes could be employed in the formation of homo/hetero bimetallic systems. Detailed work towards synthesis and structural characterization of homo/hetero bimetallic complexes using these complexes is in progress in our laboratory.

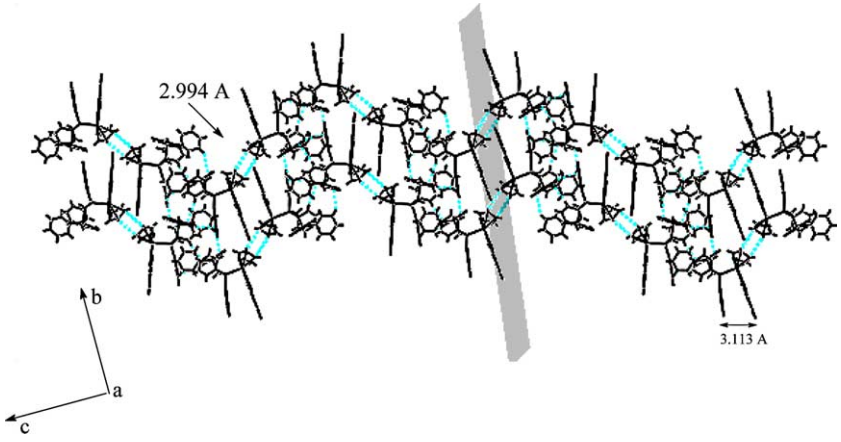

Fig. 8. Helical strands of the complex **4** showing C–H···π and π–π interactions.

3. Experimental section

3.1. Materials and physical measurements

All the synthetic manipulations were performed under oxygen free nitrogen atmosphere. The solvents were dried and distilled before use following the standard procedures. Triphenyl phosphine, triphenyl arsine, triphenyl stibine, hydrated ruthenium(III) chloride, 1,2-bis(diphenyl-phosphino)methane and ammonium tetrafluoroborate (all Aldrich) were used as received. The ligands pyridine-2-carbaldehyde azine (paa) and *p*-phenylene-bis(picoline)aldimine (pbp) and the precursor complexes $[Ru(\eta^5\text{-}C_5H_5)Cl(PPh_3)_2]$ and $[Ru(\eta^5\text{-}C_5H_5)Cl(dppm)]$ were prepared and purified following the literature procedures [7,12,18].

Elemental analyses of the complexes were performed at Sophisticated Analytical Instrument Facility, Central Drug Research Institute, Lucknow. Infrared spectra were recorded on a Perkin–Elmer-577 spectrophotometer. NMR spectra on room temperature were recorded on a Bruker-DRX300 MHz spectrometer with tetramethyl silane as an internal standard. Electronic and emission spectra of the complexes were obtained on a Shimadzu UV-1601 and Perkin–Elmer-LS 55 Luminescence spectrometer, respectively. The FAB mass spectra were recorded on a JEOL SX 102/DA 6000 mass spectrometer using Xenon (6 kV, 10 mA) as the FAB gas. The accelerating voltage was 10 kV and the spectra were recorded at room temperature with *m*-nitrobenzyl alcohol as the matrix. Electrochemical data were acquired on a PAR model 273A electrochemistry system at a scan rate of 50 mV s^{-1}. The sample solutions (10^{-4} M) were prepared in purified acetonitrile containing $NEt_4^+ClO_4^-$ (0.1 M) as a supporting electrolyte. Solution was deoxygenated by bubbling nitrogen for about 20 min in each experiment. Platinum wire working and auxiliary electrodes and an aqueous saturated calomel reference electrode were used in a three-electrode configuration.

3.2. Syntheses

3.2.1. $[Ru(\eta^5\text{-}C_5H_5)(PPh_3)(\kappa^2\text{-}paa)]BF_4$ (1)

A suspension of $[Ru(\eta^5\text{-}C_5H_5)Cl(PPh_3)_2]$ (0.727g, 1 mmol) in methanol (60 ml) was treated with pyridine-2-carbaldehyde azine (paa) (0.420 mg, 2 mmol) and the resulting suspension was heated under reflux for about 10 h. The complex $[Ru(\eta^5\text{-}C_5H_5)Cl(PPh_3)_2]$ slowly dissolved and gave a dark brown solution. It was cooled to room temperature and filtered through celite to remove any solid impurities. A saturated solution of NH_4BF_4 in methanol (25 ml) was added to the filtrate, concentrated to about 25 ml at reduced pressure and was left in refrigerator for slow crystallization. In a couple of days, crystalline product was obtained, which was separated by filtration, washed with methanol, diethyl ether, and dried in vaccuo. Yield: 0.549 g (75%). Anal. Calc. for $BC_{35}F_4H_{30}N_4PRu$: C, 57.93; H, 4.13; N, 7.71. FAB-MS *m/z*: 639(639) $[RuCp(paa)(PPh_3)]^+$; 376(377) $[RuCp(paa)]^+$. ^1H NMR (δ ppm, CDCl3, 300 MHz, 298 K): 9.54 (d, 4.8 Hz), 9.02 (s), 8.77 (d, 4.5 Hz), 8.01 (d, 6.3 Hz), 7.88 (t, 6.9 Hz), 7.65 (t, 3.6 Hz), 7.46 (t, 5.2 Hz), 7.31 (m), 4.89 (s). $^{31}P\{^1H\}$ (δ ppm, CDCl3, 120 MHz, 300 K): 48.15. UV–Vis {$CHCl_3$, λ_{max} nm (ϵ)}: 461 (5.9×10^3), 314 (3.7×10^4), 292 (3.8×10^4). Found: C, 57.82; H, 4.22; N, 7.69%.

3.2.2. $[Ru(\eta^5\text{-}C_5H_5)(AsPh_3)(\kappa^2\text{-}paa)]BF_4$ (2)

Complex **2** was prepared by the same procedure as described for the complex **1** from the reaction of $[Ru(\eta^5\text{-}C_5H_5)Cl(AsPh_3)_2]$ (0.406 g, 0.5 mmol) in methanol (30 ml) with pyridine-2-carbaldehyde azine (paa) (0.210 g, 1 mmol). The complex separated as brownish black crystals after the addition of saturated solution of NH_4BF_4 in methanol. Yield: 0.261 g (68%). Anal. Calc. for $AsBC_{35}F_4H_{30}N_4Ru$: C, 54.68; H, 3.90; N, 7.29. ^1H NMR (δ ppm, CDCl3, 300 MHz, 298 K): 9.59 (d, 4.3 Hz), 8.92 (s), 8.67 (d, 4.5 Hz), 8.21 (d, 5.3 Hz), 7.82 (t, 5.4 Hz), 7.65 (t, 3.9 Hz), 7.31 (m), 4.87 (s). UV–Vis {$CHCl_3$, λ_{max} nm (ϵ)}: 464 (8.2×10^3), 352 (1.2×10^4), 286 (1.3×10^4). Found: C, 54.60; H, 3.87; N, 7.26%.

3.2.3. $[Ru(\eta^5\text{-}C_5H_5)(SbPh_3)(\kappa^2\text{-}paa)]BF_4$ (3)

Complex **3** was prepared by following the above starting from $[Ru(\eta^5\text{-}C_5H_5)Cl(SbPh_3)_2]$ (453.5 mg, 0.5 mmol) in methanol (30 ml) with pyridine-2-carbaldehyde azine (paa) (210 mg, 1 mmol). The complex separated as dark tan powder after the addition of saturated solution of NH_4BF_4 in methanol. Yield: 0.281 g (69%). Anal. Calc. for $BC_{35}F_4H_{30}N_4RuSb$: C, 51.47; H, 3.67; N, 6.86. ^1H NMR (δ ppm, CDCl3, 300 MHz, 298 K): 9.54 (d, 4.6 Hz), 9.12 (s), 8.77 (d, 4.5 Hz), 8.15 (d, 5.6 Hz), 7.83 (t, 5.9 Hz), 7.45 (t, 3.2 Hz), 7.31 (m), 4.79(s). UV–Vis {$CHCl_3$, λ_{max} nm (ϵ)}: 474 (8.7×10^3), 362 (1.1×10^4), 302 (1.3×10^4). Found: C, 51.50; H, 3.60; N, 6.78%.

3.2.4. $Ru(\eta^5\text{-}C_5H_5)(\kappa^1\text{-}dppm)(\kappa^2\text{-}paa)]BF_4$ (4)

It was prepared following the above procedure from reaction of $[Ru(\eta^5\text{-}C_5H_5)(\kappa^2\text{-}dppm)Cl]$ (0.585 g, 1 mmol) with pyridine-2-carbaldehyde azine (paa) (0.210 mg, 2 mmol) in methanol (60 ml). It was isolated as red brown crystals. Yield: 0.593 g, (70%). Anal. Calc. for $BC_{42}F_4H_{37}N_4P_2Ru$: C, 59.50; H, 4.37; N, 6.61. FAB-MS *m/z*: 760(761) $[RuCp(paa)(dppm)]^+$; 551(551) $[RuCp(dppm)]^+$. ^1H NMR (δ ppm, CDCl3, 300 MHz, 298 K): 9.64 (d, 4.3 Hz), 9.14 (s), 8.77 (d, 4.7 Hz), 8.01 (d, 6.3 Hz), 7.86 (t, 6.9 Hz), 7.65 (t, 3.6 Hz), 7.31 (m), 4.97(s); $^{31}P\{^1H\}$ (δ ppm, CDCl3, 120 MHz, 300 K): –26.5 (d), 41.0 (d). UV–Vis {$CHCl_3$, λ_{max} nm (ϵ)}: 470

(5.4×10^3), 317 (3.8×10^4), 289 (3.6×10^3). Found: C, 59.34; H, 4.52; N, 6.47%.

3.2.5. $Ru(\eta^5\text{-}C_5H_5)(\kappa^1\text{-}dppm)(\kappa^2\text{-}pbp)]BF_4$ (5)

This complex was prepared by reaction of [Ru(η^5-C_5H_5)(κ^2-dppm)Cl] (0.585 g, 1 mmol) with *p*-phenylene-bis(picoline)aldimine (pbp) (0.286 g, 1 mmol) in methanol (30 ml). The crystals were separated by filtration, washed with methanol, diethyl ether and dried in vaccuo. Yield: 0.655 g (71%). Anal. Calc. for $BC_{48}F_4H_{41}N_4P_2Ru$: C, 62.41; H, 4.44; N, 6.07. ^{1}H NMR (δ ppm, CDCl3, 300 MHz, 298 K): 8.78 (d, 4.7Hz), 8.63 (s), 8.43 (d, 5.4Hz), 7.91 (t, 4.2 Hz) 7.22 (m), 6.98 (d, 4.1 Hz), 5.08 (s). $^{31}P\{^1H\}$ (δ ppm, CDCl3, 120 MHz, 300 K): –27.5 (d), 42.6 (d). UV–Vis {$CHCl_3$, λ_{max} nm (ϵ)}: 461 (6.8×10^3), 315 (4.3×10^4), 292 (4.3×10^3). Found: C, 62.50; H, 4.62; N, 6.27%.

3.3. X-ray crystallographic study

Crystals suitable for single crystal X-ray analyses for the complex [(η^5-C_5H_5)Ru(κ^2-paa)(PPh_3)] (**1**) and [(η^5-C_5H_5)Ru(κ^2-paa)(κ^1-dppm)] (**4**) were grown from CH_2Cl_2/petroleum ether (40–60 °C) at room temperature. Preliminary data on the space group and unit cell dimensions as well as intensity data were collected on Bruker SMART APEX 3-circle diffractometer with CCD area detector at the Servicio Central de Ciencia y Tecnología de la Universidad de Cádiz, λ (Mo Kα) = 0.71073 Å, μ(Mo Kα) = 0.581(**1**) and 0.531(**4**) mm^{-1} radiation. Structure was solved by direct methods [19]. Refinement on F^2 concluded with the values R(all) = 0.0958 and 0.0783, GOF = 0.995 and 1.051, respectively, for complexes **1** and **4**. All non-hydrogen atoms were anisotropically refined. The hydrogen atoms were geometrically calculated and refined using the SHELX riding model. Minimum and maximum residual electron density peaks were −0.31 and +0.46, −0.83, 1.0 e $Å^{-3}$ for complexes **1** and **4**, respectively. The computer programme PLATON was used for analysing the interaction and stacking distances [19].

4. Supporting material

Crystallographic data for the structural analysis of complexes **1** and **4** are available in CIF format. This material is available free of charge via the Internet. CCDC reference numbers are 233924 and 233925 for complex **1** and **4**, respectively.

Acknowledgements

Thanks are due to Department of Science and Technology, Ministry of Science and Technology, New Delhi for Financial Assistance (SP/S1/F-04/2000). We also thank to the Head, SAIF, Central Drug Research Institute, Lucknow, for providing analytical and spectral facilities and The Head, Department of Chemistry, A.P.S. University, Rewa for extending laboratory facilities.

References

[1] (a) R.D. Adams, F.A. Cotton, Catalysis by Di and Polynuclear Complexes, Wiley-VCH, New York, 1998;
(b) P. Braunstein, J. Rose, 2nd ed., in: E.W. Abel, F.G.A. Stone, G. Wilkinson (Eds.), Comprehensive Organometallic Chemistry, vol. 10, Pergmon Press, Oxford, 1995 (Chapter 7).

[2] (a) L. Roecker, T.J. Meyer, J. Am. Chem. Soc. 109 (1987) 746;
(b) V.J. Catalono, R.A. Heck, C.E. Immoos, A. Ohman, M.G. Hill, Inorg. Chem. 37 (1998) 2150;
(c) M. Navarro, W.F. De Giovani, J.R. Romero, J. Mol. Catal. A: Chem. 135 (1998) 249;
(d) A. Gerli, J. Reedijk, M.T. Lakin, A.L. Spek, Inorg. Chem. 34 (1995) 1836;
(e) E.P. Kelson, L.M. Henling, W.P. Schaefer, J.A. Labinger, J.E. Bercaw, Inorg. Chem. 32 (1993) 2863;
(f) K.Y. Wong, V.W. Yam, W.W. Lee, Electrochim. Acta 37 (1992) 2645;
(g) C.M. Che, T.F. Lai, K.Y. Wong, Inorg. Chem. 26 (1987) 2289.

[3] (a) S.D. Orth, M.R. Terry, K.A. Abboud, B. Dodson, L. McElwee-White, Inorg. Chem. 35 (1996) 916;
(b) Y. Yang, K.A. Abboud, L. McElwee-White, J. Chem. Soc., Dalton Trans. (2003) 4288.

[4] (a) C.P. Liu, Y.-S. Wen, L.-K. Liu, Organometallics 16 (1997) 155;
(b) M.L. Man, Z. Zhou, S.M. Ng, C.P. Lau, J. Chem. Soc., Dalton Trans. (2003) 3727.

[5] (a) E.A. Meyer, R.K. Castellano, F. Diederich, Angew. Chem. Int. Ed. 1210 (2003) 42;
(b) D. Braga, P.J. Dyson, F. Grepioni, B.F.G. Johnson, Chem. Rev. 94 (1994) 1585.

[6] (a) D. Braga, F. Grepioni, G.R. Desiraju, J. Organomet. Chem. 548 (1997) 33;
(b) S. Aime, E. Diana, R. Gobetto, M. Milanesio, E. Valls, D. Viterbo, Organometallics 21 (2002) 50.

[7] (a) M.I. Bruce, A.G. Swincer, Aust. J. Chem. 33 (1980) 1471;
(b) M. Ghedini, M. Longeri, F. Neve, J. Chem. Soc., Dalton Trans. (1986) 2669;
(c) M. Ghedini, A.M.M. Langfredi, F. Neve, A. Tripicchio, J. Chem. Soc., Chem. Commun. (1987) 847.

[8] (a) D.S. Pandey, R.L. Mishra, U.C. Agarwala, Indian J. Chem. 31A (1991) 41;
(b) D.K. Gupta, A.N. Sahay, D.S. Pandey, N.K. Jha, P. Sharma, G. Espinosa, A. Cabrera, M.C. Puerta, P. Valerga, J. Organomet. Chem. 568 (1998) 13.

[9] (a) V. Gutmann, The Donor Acceptor Approach to Molecular Interactions, Plenum Press, New York, 1980;
(b) A.B.P. Lever, Inorganic Electronic Spectroscopy, second ed., Elsevier, Amsterdam, 1984;
(c) C. Reichardt, Angew. Chem., Int. Ed. Eng. 18 (1979) 98;
(d) S. Ernst, W. Kaim, J. Am. Chem. Soc. 108 (1986) 3578.

[10] (a) J.C. Curtis, B.P. Sullivan, T.J. Meyer, Inorg. Chem. 22 (1983) 224;
(b) J. Granifo, M.E. Vargas, E.S. Dodsworth, D.H. Farrar, S.S. Fielder, A.B.P. Lever, J. Chem. Soc., Dalton Trans. (2003) 3727–3735.

[11] B.P. Sullivan, D.J. Salmon, T.J. Meyer, Inorg. Chem. 17 (1978) 3334.
[12] (a) W.J. Stratton, D.H. Busch, J. Am. Chem. Soc. 80 (1958) 1286;
(b) M.-A. Haga, K. Koizumi, Inorg. Chim. Acta 104 (1985) 47.
[13] M.I. Bruce, F.S. Wong, B.W. Skelton, A.H. White, J. Chem. Soc., Dalton Trans. (1981) 1398.
[14] (a) J. Trotter, Acta Crystallogr. 16 (1963) 571;
(b) Y.S. Sohn, A.W. Schlueter, D.N. Hendrickson, H.B. Gray, Inorg. Chem. 13 (1974) 301.
[15] (a) K.J. Guggenberger, Inorg. Chem. 12 (1973) 1317;
(b) E. Becker, C. Slugovc, E. Ruba, C. Standfest-Hauser, K. Mereiter, R. Schmidt, K. Kirschner, J. Organometal. Chem. 649 (2002) 55.
[16] (a) N.T. Huang, W.T. Pennington, J.N. Petersen, Acta Crystallogr., Sect. C 47 (1991) 2011;
(b) A. Escuer, R. Vicente, T. Comas, J. Ribas, M. Gomez, X. Solans, D. Gatteschi, C. Zanchini, Inorg. Chim. Acta 181 (1991) 51;
(c) W.S. Sheldrick, H.S. Hagen-Eckhard, S. Heeb, Inorg. Chim. Acta 206 (1993) 15;
(d) W. Luginbuehl, P. Zbinden, P.A. Pittet, T. Armbruster, H.B. Buergi, A.E. Merbach, A. Ludi, Inorg. Chem. 30 (1991) 2350;
(e) A.J. Davenport, D.L. Davies, J. Fawcett, S.A. Garratt, D.R. Russell, J. Chem. Soc., Dalton Trans. (2000) 4432.
[17] (a) D. Braga, F. Grepioni, Chem. Commun. (1996) 571;
(b) T. Steiner, Angew. Chem., Int. Ed. Engl. 41 (2002) 48;
(c) G.R. Desiraju, T. Steiner, The Weak Hydrogen Bond in Structural Chemistry and Biology, Oxford University Press, Oxford, 1999;
(d) K. Ozeki, N. Sakabe, J. Tanaka, Acta Crystallogr., Sect. B 25 (1969) 1038;
(e) H. Suezawa, T. Yoshida, S. Ishihara, Y. Umezawa, M. Nishio, Cryst. Eng. Commun. 5 (2003) 514.
[18] G.S. Ashby, M.I. Bruce, I.B. Tomkins, R.C. Wallis, Aust. J. Chem. 32 (1979) 1003.
[19] (a) G.M. Sheldrick, SHELX-97: Programme for Refinement of Crystal Structures, University of Gottingen, Gottingen, Germany, 1997;
(b) PLATON, A.L. Spek, Acta Crystallogr., Sect. A 46 (1990) C34.